Japanese Journal of Applied Physics **49** (2010) 070206 **RAPID COMMUNICATION**

Optimization of Device Structures for Bright Blue Semipolar $(10\bar{1}\bar{1})$ Light Emitting Diodes via Metalorganic Chemical Vapor Deposition

Yuji Zhao[1], Junichi Sonada[2], Ingrid Koslow[2], Chih-Chien Pan[2], Hiroaki Ohta[2*],
Jun-Seok Ha[2], Steven P. DenBaars[1,2], and Shuji Nakamura[1,2]

[1]*Electrical and Computer Engineering Department, University of California, Santa Barbara, CA 93106, U.S.A.*
[2]*Materials Department, University of California, Santa Barbara, CA 93106, U.S.A.*

Received April 16, 2010; accepted May 19, 2010; published online July 5, 2010

The device structures of semipolar $(10\bar{1}\bar{1})$ GaN blue light emitting diodes (LEDs) were optimized to achieve high power and high efficiency via metalorganic chemical vapor deposition (MOCVD). The quantum well (QW) width, barrier thickness and last barrier (LB) thickness were varied in order to optimize device performances and achieve the best growth conditions. Additional optimization methods such as Mg doping for the LB and p+ contact layers were also investigated. This study resulted in a LED with an output power of 22.75 mW and an external quantum efficiency (EQE) of 39.5% at a driving current of 20 mA, which is a significant improvement over previous results.

DOI: 10.1143/JJAP.49.070206

Semipolar nitride light emitting diodes (LEDs) have attracted considerable attention because they have the potential to outperform current commercially available *c*-plane optoelectronic devices, due to their lack of polarization-related electric fields inside the quantum wells (QWs).[1–5] *C*-plane devices grown along the polar (0001) *c*-axis direction via metalorganic chemical vapor deposition (MOCVD)[1] suffer from these large internal electric fields due to discontinuities in both spontaneous and piezoelectric polarization at the heterointerface. This leads to the quantum confined Stark effect (QCSE), where the electrons and holes are separated in the quantum wells and the radiative recombination rate is reduced.[2–5] Devices grown on nonpolar planes such as the $(1\bar{1}00)$ *m*-plane, $(11\bar{2}0)$ *a*-plane,[6,7] as well as devices on the $(11\bar{2}2)$ and $(10\bar{1}\bar{1})$ semipolar planes have been demonstrated with eliminated or reduced polarization fields.[6–16] However, the presence of a high density of threading dislocations (TDs) and basal plane stacking faults (SFs) limited the performance of first generation nonpolar and semipolar LEDs.[17,18]

Recently, the performances of nonpolar and semipolar LEDs have been significantly improved by the availability of low defect density free standing GaN bulk substrates.[19–25] Several experimental results on nonpolar and semipolar LEDs on bulk GaN substrates have been reported by various groups. For the semipolar $(11\bar{2}2)$ plane, blue, green and amber InGaN/GaN LEDs were first reported by Funato *et al.* with a relatively low output power and external quantum efficiency (EQE).[21] Sato *et al.* improved the device performance in the green[22] and yellow regions.[23] For the semipolar $(10\bar{1}\bar{1})$ plane, Tyagi *et al.* first reported violet InGaN/GaN LED ($300 \times 300\,\mu m^2$) grown on a bulk GaN substrate with an output power of 20.58 mW and an EQE of 33.91% at a driving current of 20 mA.[24] Later, devices in the blue region ($200 \times 550\,\mu m^2$) were also reported with an output power and EQE of 16.21 mW and 29% respectively, at 20 mA, which were the highest values published until now for semipolar blue LEDs.[25] Although there were several reports on semipolar InGaN/GaN LED performances, the MOCVD growth conditions and device structures have never been fully explored.

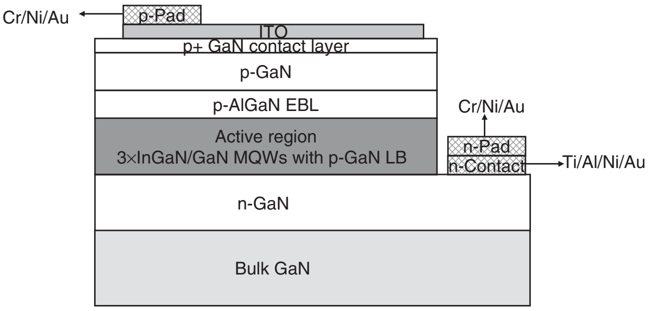

Fig. 1. Schematic views of the semipolar $(10\bar{1}\bar{1})$ LED device structures.

In this paper, we carried out a comprehensive study on growth conditions and device structures on the $(10\bar{1}\bar{1})$ semipolar plane to optimize LED performances around the 450 nm blue region. The effects of well width, barrier thickness and last barrier (LB) thickness were investigated. The optimization results are similar to those on *m*- and *c*-plane devices.[1,26] Additionally, Mg doping for the LB and p+ contact layer were also studied as alternate optimization methods. Finally, utilizing this optimized structure, we report the performance of a high power and high efficiency blue LED.

The LED structures were homoepitaxially grown by conventional MOCVD on free standing $(10\bar{1}\bar{1})$ GaN substrates, supplied by Mitsubishi Chemical Corporation. The typical device structure started with a 1 µm Si-doped n-type GaN layer, followed by the active region, which consisted of three periods of undoped GaN barriers and InGaN quantum wells (QWs) ending with a Mg-doped GaN last barrier (LB). A Mg-doped 16 nm $Al_{0.15}Ga_{0.85}N$ electron blocking layer (EBL) was grown after the last barrier, followed by a 50 nm p-type GaN layer and a 10 nm p+ GaN contact layer. A schematic of the device structure is shown in Fig. 1.

To optimize the active region, we changed three variables, which were barrier thickness, last barrier thickness, and well width, respectively. The room-temperature (RT) electroluminescence (EL) data are summarized in Fig. 2. All the devices were grown under such conditions that their wavelengths were around 440 nm, as is shown in Figs. 2(a)–2(c).

---

[*] E-mail address: ohta@engineering.ucsb.edu

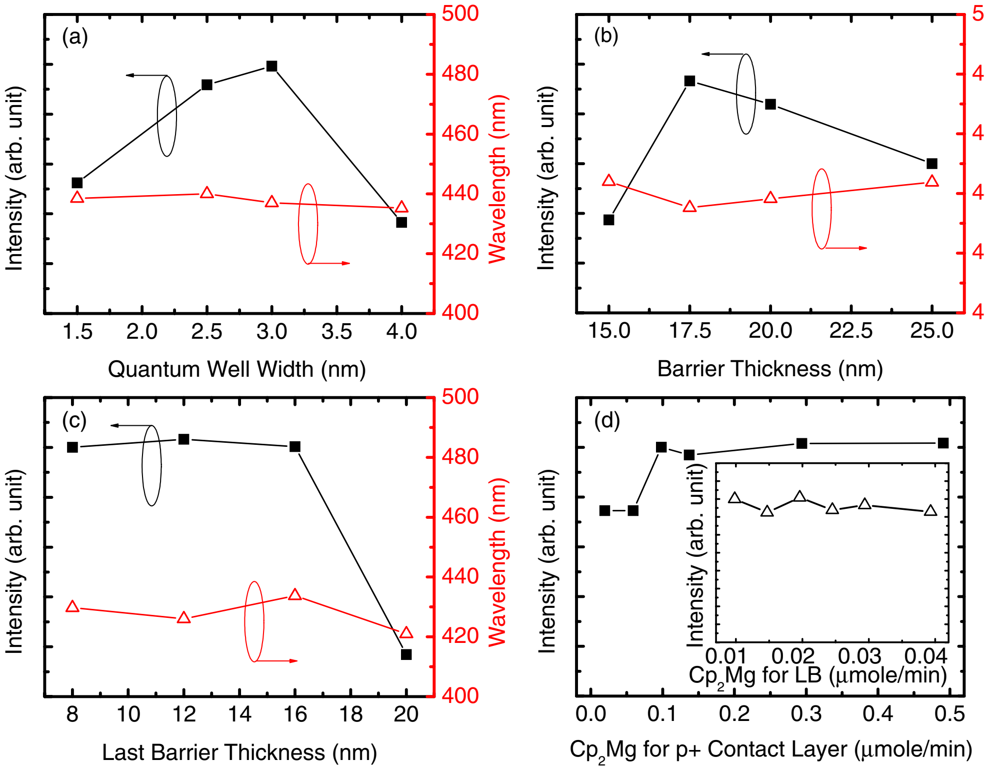

Fig. 2. (Color online) The dependence of the EL intensity and wavelength on (a) quantum well width, (b) Barrier thickness, (c) last barrier (LB) thickness and (d) Mg doping for LB and p+ contact layer for semipolar LEDs.

Figure 2(a) shows the dependence of EL intensity and wavelength on the well width of the LEDs. The EL intensity increased significantly between well widths of 1.5 to 3 nm, but it started to decrease when the well width was further increased above 3 nm. A similar tendency of EL intensity was observed in the case of change of barrier thickness, where the EL intensity shows a peak for a 17.5 nm thick barrier [Fig. 2(b)]. These two results demonstrate that either a too narrow well or a too thin barrier is not sufficient to confine the injected carriers within the wells, thus reducing the radiative recombination rate. These are consistent results with those of Lin *et al.* for *m*-plane devices.[26] Although Kim *et al.* reported an advantage of growing thick QWs for nonpolar devices due to the absence of the QCSE,[27] we found it is less beneficial for semipolar devices to grow QWs that are wider than 3 nm. This result is similar to optimum well widths grown on *c*-plane LEDs, which are typically ~2.5 nm.[1] We attribute this to low radiative efficiency for thicker QWs, as thicker QWs will result in lower carrier concentrations and reduce the radiative recombination. On the other hand, poor structural quality of the thicker InGaN QWs may also be the cause, as defects such as dislocations will act as nonradiative centers which are detrimental to radiative efficiency.

Figure 2(c) demonstrates the dependence of EL intensity on the LB thickness. The EL intensity is less sensitive to the thickness of the last barrier, remaining fairly constant for LB thickness between 8 and 16 nm, and dropping when the thickness is increased to 20 nm. It is possible that the cause of this final drop is due to the thicker barriers hindering injection of holes into the quantum well from the p-GaN.

Additionally, Fig. 2(d) shows the dependence of EL intensity on Mg doping for the LB and p+ contact layer. It is clear that EL intensity was relatively insensitive to Mg doping of the LB, while in the p+ contact layer, there is an abrupt increase in EL intensity at a Cp$_2$Mg flow of around 0.05 μmol/min. A systematic study for doping on device performance is under investigation.

For the $(10\bar{1}\bar{1})$ LED fabrication, an indium tin oxide current spreading layer was deposited by electron beam evaporation. A rectangular mesa pattern (500 × 2000 μm^2) was formed by conventional lithography and chlorine-based inductively coupled plasma (ICP) etching. Ti/Al/Ni/Au n-type contacts and Cr/Ni/Au pads were deposited by electron beam evaporation and a conventional lift-off process. The fabrication steps did not involve any intentional light extraction techniques. A new LED structure with improved light extraction efficiency is under investigation and will be published in another paper. The LEDs were then diced and packaged using a transparent stand packaging method, the details of which are described elsewhere.[28] Room temperature (RT) EL measurements under pulsed conditions with a duty cycle of 1% were performed in an integrating sphere. Figure 3 shows the light-output-power vs current (*L*–*I*) and external quantum efficiency vs current (EQE–*I*) curves for a typical optimized $(10\bar{1}\bar{1})$ LED under such conditions. At a forward current of 20 mA, the semipolar LED has an output power of 22.75 mW and an EQE of 39.5%. The LED demonstrates a small efficiency droop with an EQE and output power at 100 mA of 38.4% and 110.50 mW respectively, which are higher than the numbers in previous publications.

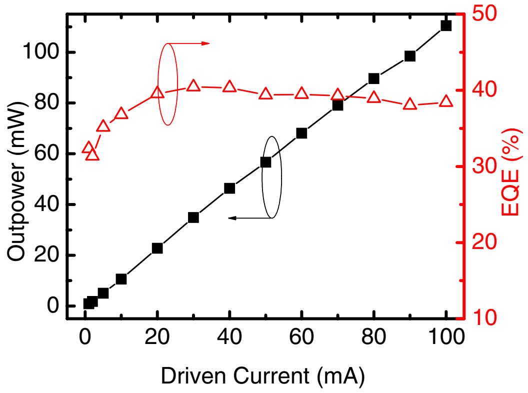

Fig. 3. (Color online) The light-output-power vs current (*L*–*I*) and external quantum efficiency vs current (EQE–*I*) curves for a typical optimized $(10\bar{1}\bar{1})$ LED under pulsed conditions.

In summary, the device structures have been optimized for semipolar $(10\bar{1}\bar{1})$ LEDs to achieve high power and high efficiency devices. Well width, barrier thickness as well as LB thickness were optimized, and additionally Mg doping for LB and p+ contact layer were studied. The optimization resulted in a bright LED with 22.75 mW output power and 39.5% EQE at 20 mA, which is the highest reported value for the $(10\bar{1}\bar{1})$ plane. Special nonpolar/semipolar LED structures with high light extraction efficiency are under study and devices with improved performance can be expected in the near future.

Acknowledgements The authors acknowledge the support of Solid State Lighting and Energy Center at UCSB. A portion of this work was done in the UCSB nanofabrication facility, part of the NSF funded NNIN network.

1) S. Nakamura and G. Fasol: *The Blue Laser Diode* (Springer, Heidelberg, 1997) 2nd ed., p. 193.
2) F. Bernardini and V. Fiorentini: Phys. Status Solidi B **216** (1999) 391.
3) A. Hangleiter, J. S. Im, H. Kollmer, S. Heppel, J. Off, and F. Scholz: MRS Internet J. Nitride Semicond. Res. **3** (1998) 15.
4) A. E. Romanov, T. J. Baker, S. Nakamura, and J. S. Speck: J. Appl. Phys. **100** (2006) 023522.
5) S. Chichibu, T. Azuhata, T. Sota, and S. Nakamura: Appl. Phys. Lett. **69** (1996) 4188.
6) P. Walterweit, O. Brandt, A. Trampert, H. T. Grahn, J. Menniger, M. Ramsteiner, M. Reiche, and K. H. Ploog: Nature **406** (2000) 865.
7) C. Q. Chen, V. Adivarahan, J. W. Yang, M. Shatalov, E. Kuokstis, and M. A. Khan: Jpn. J. Appl. Phys. **42** (2003) L1039.
8) R. Sharma, P. M. Pattison, H. Masui, R. M. Farrel, T. J. Baker, B. A. Haskell, F. Wu, S. P. DenBaars, J. S. Speck, and S. Nakamura: Appl. Phys. Lett. **87** (2005) 231110.
9) H. Masui, T. J. Baker, R. Sharma, P. M. Pattison, M. Iza, H. Zhong, S. Nakamura, and S. P. DenBaars: Jpn. J. Appl. Phys. **45** (2006) L904.
10) H. Masui, T. J. Baker, M. Iza, H. Zhong, S. Nakamura, and S. P. DenBaars: J. Appl. Phys. **100** (2006) 113109.
11) A. Chitnis, C. Chen, V. Adivarahan, M. Shatalov, E. Kuokstis, V. Mandavilli, J. Yang, and M. A. Khan: Appl. Phys. Lett. **84** (2004) 3663.
12) A. Chakraborty, B. A. Haskell, S. Keller, J. S. Speck, S. P. DenBaars, S. Nakamura, and U. K. Mishra: Appl. Phys. Lett. **85** (2004) 5143.
13) A. Chakraborty, B. A. Haskell, H. Masui, S. Keller, J. S. Speck, S. P. DenBaars, S. Nakamura, and U. K. Mishra: Jpn. J. Appl. Phys. **45** (2006) 739.
14) M. Funato, M. Ueda, Y. Kawakami, Y. Narukawa, T. Kosugi, M. Takahashi, and T. Mukai: Jpn. J. Appl. Phys. **45** (2006) L659.
15) A. Chakraborty, B. A. Haskell, S. Keller, J. S. Speck, S. P. DenBaars, S. Nakamura, and U. K. Mishra: Jpn. J. Appl. Phys. **44** (2005) L173.
16) A. Chakraborty, T. J. Baker, B. A. Haskell, F. Wu, S. Keller, J. S. Speck, S. P. DenBaars, S. Nakamura, and U. K. Mishra: Jpn. J. Appl. Phys. **44** (2005) L945.
17) T. J. Baker, B. A. Haskell, F. Wu, P. T. Fini, J. S. Speck, and S. Nakamura: Jpn. J. Appl. Phys. **44** (2005) L920.
18) T. J. Baker, B. A. Haskell, F. Wu, J. S. Speck, and S. Nakamura: Jpn. J. Appl. Phys. **45** (2006) L154.
19) M. Schmidt, K. Kim, H. Sato, N. Fellows, H. Masui, S. Nakamura, S. P. DenBaars, and J. S. Speck: Jpn. J. Appl. Phys. **46** (2007) L126.
20) K. Okamoto, H. Ohta, D. Nakagawa, M. Sonobe, J. Ichihara, and H. Takasu: Jpn. J. Appl. Phys. **45** (2006) L1197.
21) M. Funato, M. Ueda, Y. Kawakami, Y. Narukawa, T. Kosugi, M. Takahashi, and T. Mukai: Jpn. J. Appl. Phys. **45** (2006) L659.
22) H. Sato, A. Tyagi, H. Zhong, N. Fellows, R. B. Chung, M. Saito, K. Fujito, J. S. Speck, S. P. DenBaars, and S. Nakamura: Phys. Status Solidi: Rapid Res. Lett. **1** (2007) 162.
23) H. Sato, R. B. Chung, H. Hirasawa, N. Fellows, H. Masui, F. Wu, M. Saito, K. Fujito, J. S. Speck, S. P. DenBaars, and S. Nakamura: Appl. Phys. Lett. **92** (2008) 221110.
24) A. Tyagi, H. Zhong, N. Fellows, M. Iza, J. S. Speck, S. P. DenBaars, and S. Nakamura: Jpn. J. Appl. Phys. **46** (2007) L129.
25) H. Zhong, A. Tyagi, N. Fellows, F. Wu, R. B. Chung, M. Saito, K. Fujito, J. S. Speck, S. P. DenBaars, and S. Nakamura: Appl. Phys. Lett. **90** (2007) 233504.
26) Y. Lin, A. Chakraborty, S. Brinkley, H. C. Kuo, T. Melo, K. Fujito, J. S. Speck, S. P. DenBaars, and S. Nakamura: Appl. Phys. Lett. **94** (2009) 261108.
27) K. C. Kim, M. C. Schmidt, H. Sato, F. Wu, N. Fellows, Z. Jia, M. Saito, S. Nakamura, S. P. DenBaars, and J. S. Speck: Appl. Phys. Lett. **91** (2007) 181120.
28) C. C. Pan, I. Koslow, J. Sonoda, H. Ohta, J. S. Ha, S. Nakamura, and S. P. DenBaars: to be published in Jpn. J. Appl. Phys.